Colloid Polym Sci 278:143–149 (2000)
© Springer-Verlag 2000

ORIGINAL CONTRIBUTION

L.P. Novaki
P.A.R. Pires
O.A. El Seoud

Fourier transform-IR and ^{1}H NMR studies on the structure of water solubilized by reverse aggregates of calcium bis(2-ethylhexyl) sulfosuccinate in organic solvents

Received: 12 July 1999
Accepted: 30 August 1999

Presented at the 39th General Meeting of the Kolloid-Gesellschaft, Würzburg, 27–30 September, 1999

L.P. Novaki · P.A.R. Pires
O. A. El Seoud (✉)
Instituto de Química
Universidade de São Paulo
C.P. 26.077, 05599-970
São Paulo, S.P., Brazil
E-mail: elseoud@iq.usp.br
Fax: +55-11-8183874

Abstract The structure of water solubilized by reverse aggregates of calcium bis(2-ethylhexyl) sulfosuccinate in deuterobenzene and toluene has been probed by Fourier transform-IR and ^{1}H NMR spectroscopies. The ν_{OD} band of solubilized HOD (4% D_2O in H_2O) has been recorded as a function of the [water]/[surfactant] molar ratio, W/S. Curve fitting of this band showed the presence of a main peak at 2550 ± 13 cm^{-1} and a small one at 2405 ± 15 cm^{-1}. As a function of increasing W/S, the frequency of the main peak decreases, its full width at half-height increases, and its area increases linearly. The ^{1}H NMR chemical shift of solubilized H_2O–D_2O mixtures at W/S = 18.1 has been measured as a function of the deuterium content of the aqueous nanodroplet. These data were used to calculate the so-called "fractionation factor" of the aggregate-solubilized water, the value of which was found to be unity. The results of both techniques show that reverse aggregate-solubilized water, although different from bulk water, does not seem to coexist in "layers" of different degrees of structure, as suggested, for example by the two-state water-solubilization model.

Key words Reverse micelles · Microemulsions · Water-in-oil · Structure of interfacial water · Fourier transform · IR and ^{1}H NMR spectroscopy of interfacial water

Introduction

Several surfactants aggregate in organic solvents of low polarity and dielectric constant (e.g., aliphatic and aromatic hydrocarbons) to form reverse micelles. These species dissolve water and aqueous solutions. The wet reverse micelles, (RMs), and the water-in-oil microemulsions (W/O μEs) formed have been used as "microreactors" for many classes of organic and inorganic reactions, including polymerization of water-soluble monomers and production of quasi monodisperse inorganic particles [1–8].

Aggregate-solubilized water is involved in, *inter alia*, hydration of the surfactant headgroup, solvation of reactants and transition states, and in electron and proton transfers. Therefore, determination of the properties of this water (e.g., its structure, microscopic polarity, and viscosity) and comparison of these properties with those of bulk water are relevant to the above-mentioned applications. The [water]/[surfactant] molar ratio (W/S) is usually used to designate the aggregates present in solution, either as RMs or as W/O μEs. In RMs the amount of solubilized water is less than the amount necessary to hydrate the surfactant headgroup. Solubilization of water beyond this W/S results in the formation of a W/O μE [8].

We are interested in studying the structure of reverse-aggregate-solubilized-water and its dependence on the nature of the surfactant headgroup [9–12]. A schematic representation of a W/O μE, showing the different types

of water that have been claimed to be present in the reverse micelles of sodium bis(2-ethylhexyl) sulfosuccinate (EtHxSS)Na is given in Fig. 1. In principle, there can be up to three "layers" within the micellar water "pool" [13–21]. The first one, W_{bound}, is at the periphery of the pool, and is made of water molecules tightly bound to the surfactant headgroup. Properties of this type of water deviate appreciably from those of bulk water. The second, intermediate "layer", $W_{intermediate}$, refers to distorted hydrogen-bonded water species, for example, cyclic dimers or higher aggregates with unfavorable hydrogen-bonds. The third, central "layer" contains bulklike water, $W_{bulklike}$, and its formation coincides with the formation of the W/O μE [14–19]. According to some authors, there is one more type of water which lies at the oil side of the interface. This interfacial water, $W_{interfacial}$, refers to "monomeric water molecules which are not bound to any other molecules or groups but are trapped between the polar headgroups of the surfactant at the interface" [20, 21]. In part, this model is based on the observation that several properties of reverse-aggregate-solubilized water show a pronounced change in the RM regime, followed by a smaller one in the W/O μE domain [8].

We report here the structure of water solubilized by reverse aggregates of calcium bis(2-ethylhexyl) sulfosuccinates [$(EtHxSS)_2Ca$] in C_6D_6 and toluene as determined by two noninvasive spectroscopic techniques. Using Fourier transform (FT)-IR spectroscopy, we have studied the dependence of the properties of ν_{OD} of solubilized HOD on W/S and have carried out peak deconvolution in order to determine the types of water present. The deuterium isotope effect on the chemical shift of solubilized H_2O–D_2O mixtures, at a constant W/S, has been used to calculate the so-called deuterium/protium "fractionation factor", φ_M, whose value bears on the structure of water within the aqueous nanodroplet [12]. Results of both techniques indicate that Fig. 1 is an oversimplification, i.e., reverse-aggregate-solubilized water does not seem to coexist in "layers" of different structures, although its properties do change continuously as a function of increasing W/S.

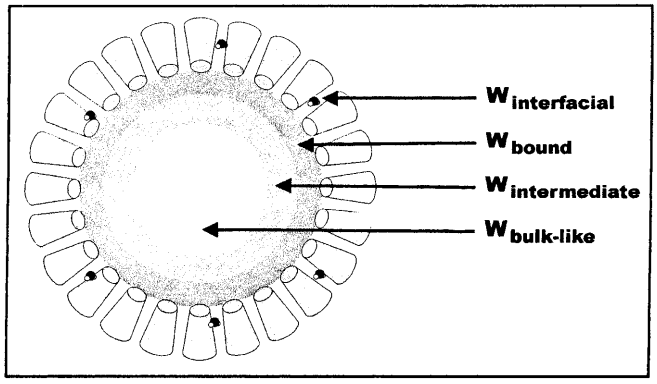

Fig. 1 Schematic representation of a water-in-oil microemulsion formed by sodium bis(2-ethylhexyl)sulfosuccinate showing the types of water which have been claimed to be present in the system. The *symbols* refer to surfactant (○) and water (●) molecules

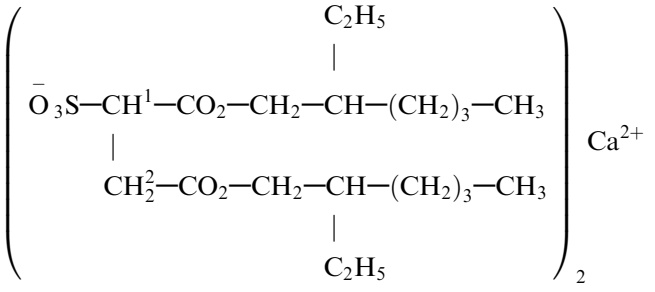

Experimental

Materials

All chemicals were obtained from Aldrich or Merck. Deuterobenzene and toluene were distilled from calcium hydride, then kept under nitrogen over activated type-4Å molecular sieves. The surfactant $(EtHxSS)_2Ca$ was prepared from the corresponding (EtHxSS)Na as given elsewhere for $(EtHxSS)_2Mg$ [11]. The extent of replacement of Na^+ by Ca^{2+} was determined by atomic absorption spectrophotometry (Perkin-Elmer model 403) and was found to be greater than 99.5%. Before use, the surfactant was dried under reduced pressure over P_2O_5 until a constant weight was obtained. Glass double-distilled H_2O was used throughout D_2O was used as received; its deuterium content was determined by ^1H NMR by using dioxane as an internal standard [22].

Methods

Surfactant stock solutions were prepared by weight: they contained solubilized H_2O, 4% D_2O in H_2O, or D_2O. Every effort was been made to ensure that these stock solutions contained the same amounts of surfactant and solvent and equivalent amounts of H_2O, 4% D_2O in H_2O, or D_2O, respectively. Typical differences in weight were less than 0.1%. This matching procedure was followed in the preparation of each sample.

FT-IR spectroscopy

The surfactant solution in toluene had a concentration of 0.2 M. The following cells from Wilmad Glass (Buena, N.J.) were used: CaF_2 (0.55 mm, 0.053 mm) and Irtran-2 (0.21 and 0.11 mm). The exact cell path length was determined by the fringe method [23]. IR spectra were recorded with a Bomem MB 100-C26 FT-IR spectrophotometer. Transmission spectra were obtained by adding together 18 spectra at 1 cm^{-1} resolution. The ν_{OD} band is superimposed on a finite background which could be approximated with the spectrum of 100% H_2O in the ν_{OD} spectral region [24, 25]. Therefore, the reference sample, at each W/S, was a surfactant solution containing matched W/S, adjusted with pure H_2O. Band deconvolution was carried out using the GRAMS/32, version 5, curve-fitting program (Galactic Industries Co., Salem, N.H.).

^{1}H NMR spectroscopy

The surfactant solution had a concentration of 0.2 M in C_6D_6. The desired atom fraction of deuterium in the water pool was obtained by weighing, in 1-ml volumetric tubes, the appropriate volumes of matched surfactant stock solutions, containing solubilized H_2O or D_2O. A Bruker DRX-500 NMR spectrometer (operating at 500.13 MHz for protons) was used. The spectra were recorded at 29.0 °C, using acquisition parameters which were adjusted to achieve a digital resolution of 0.06 Hz/datum point. The spectrometer probe temperature was periodically monitored by measuring the chemical shift difference between the singlets of a methanol reference. The probe thermal stability was assured by the observation that successive measurements of the sample chemical shift (after 10 min in the probe for thermal equilibration) were within the digital resolution limit. Chemical shifts were measured relative to the isotopic impurity singlet of C_6D_6 and were then transformed to the tetramethylsilane scale by using the known chemical shift for C_6H_6 of 7.16 ppm [26].

Results

FT-IR spectroscopy

Figure 2 shows typical ν_{OD} bands and the corresponding band deconvolution, in the 2800–2100 cm^{-1} region. Although curve fitting was carried out by considering contributions from Gaussian and Lorentzian components, our calculations showed that the bands are essentially Gaussian, in agreement with previous work on HOD in bulk aqueous phases [24, 25, 27–30] and in RMs and W/O μEs of (EtHxSS)Na, $(EtHxSS)_2Mg$, and cetyltrimethylamonium bromide [10, 11]. The quality of the fit of the ν_{OD} bands in the W/S range studied is evident from the root mean squares, 0.17 ± 0.03, and the corresponding standard errors, 0.007 ± 0.002. Sample matching by weight and the use of the appropriate reference to eliminate the contribution from the H_2O combination band at 2100 cm^{-1} resulted in a good, horizontal base line, essential for meaningful curve fitting.

The peak parameters which were measured directly from the digitized spectra are shown in Fig. 3. The dependence of the peak frequency (position of maximum absorption of the main peak. (Fig. 3A) and of the full width at half height (FWHH) of the same peak (Fig. 3B) on W/S is described by the equation

$$\mathrm{FWHH} = a + b(\mathrm{W/S}) + c(\mathrm{W/S})^2 \quad , \qquad (1)$$

where a, b, and c are regression coefficients. The correlation coefficients, CC, and the sum of the squares of the residuals, ΣQ, are 0.9958 and 3 for Fig. 3A and 0.9976 and 1.35 for Fig. 3B. In the W/S range studied (from 3.85 to 15.57) ν_{OD} and FWHH are 2550 ± 13 cm^{-1} and 155 ± 15 cm^{-1}, not far from the corresponding values reported for a saturated solution of $CaCl_2$ in HOD (2533 and 194 cm^{-1}) [27]. The linear correlation between W/S and the corresponding areas of the main peak is shown in Fig. 3C. CC and ΣQ are 0.9978 and 112, respectively.

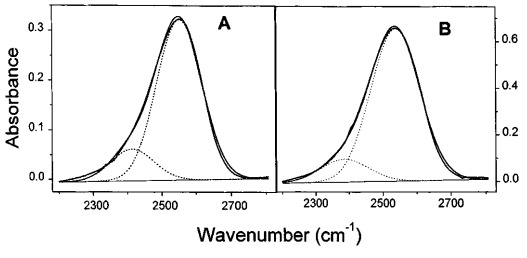

Fig. 2 Representative IR spectra and band deconvolution of the ν_{OD} peak of HOD solubilized by reverse aggregates of calcium bis(2-ethylhexyl) sulfosuccinate [*(EtHxSS)$_2$Ca*] in toluene at **A** a water/surfactant molar ratio (*W/S*) of 7.62 and **B** at W/S = 15.57.The *solid curves* correspond to recorded and calculated spectra and the *dotted ones* show Gaussian components, obtained by deconvolution

^{1}H NMR spectroscopy

For the surfactant employed, the maximum W/S (19) is similar in toluene and in C_6D_6. We used the latter

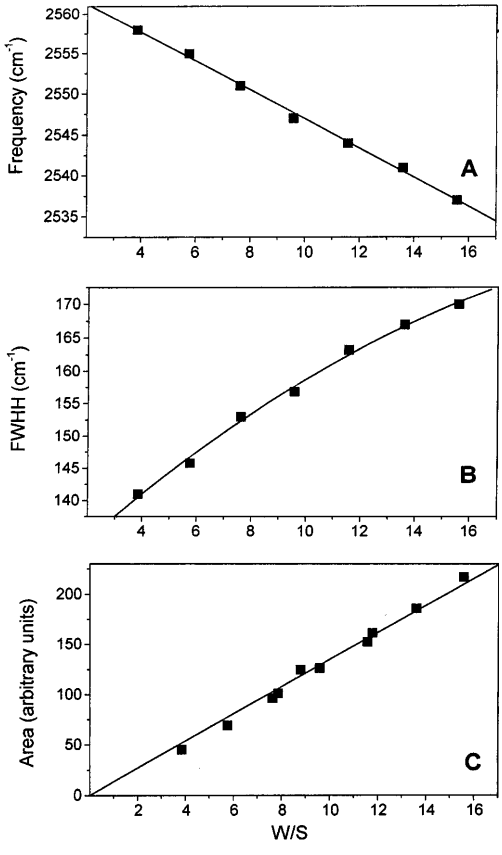

Fig. 3A–C Dependence on W/S of the characteristic properties of the principal band of ν_{OD} for $(EtHxSS)_2Ca$-solubilized HOD. **A**, **B**, and **C** show the frequency, the full width at half-height (*FWHH*) and the area, respectively

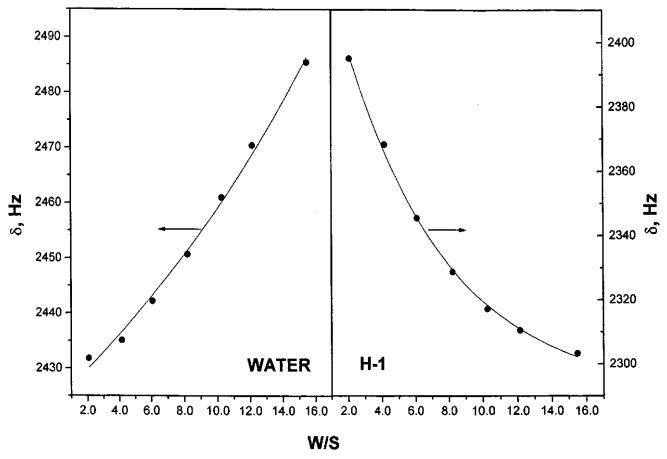

Fig. 4 Dependence of the chemical shift of solubilized H_2O and of H1 of $(EtHxSS)_2Ca$ on W/S. Surfactant concentration = 0.2 M, 500.13 MHz; T= 29.0 °C, chemical shifts are given relative to tetramethylsilane

solvent because it is convenient for carrying out ^1H NMR measurements. Figure 4 shows the dependence of the observed chemical shifts, δ_{obs}, for water and H-1 of the surfactant on W/S. The points refer to experimental date and the solid curves were plotted according to Eq. (1).

Discussion

IR and Raman spectroscopy are suitable techniques to detect different types of water at an interface. This results from the very short observation times (10^{-12}–10^{-14} s) which match the rapid time scales on which water molecules are expected to interchange with each other (between 10^{-7} and 10^{-11} s) [31]. Thus, water molecules present in different environments should show up as separate bands in the IR or Raman spectrum, provided that the difference in the vibrational energies is suitably large. Quantitative treatment of IR and Raman experimental data requires an "a priori" hypothesis on the origin of the vibrational dynamics of the system under analysis. The model suggested should fit the data accurately (i.e., with the least possible error) and should agree with chemistry. This observation is central to curve fitting of spectroscopic data [32, 33], and indeed to any problem whose solution relies on curve fitting [34].

Based on the preceding paragraph, it is expected that examination of the same system, by the same spectroscopic technique, should yield converging conclusions with regard to the number of water "layers" present within the reverse aggregate and to the relative concentration of each type. Unfortunately, this is not the case, as shown by the following IR and Raman data on RMs and W/O μEs of (EtHxSS)Na (the most extensively studied surfactant):

1. The number of water types present within the aggregate varies from 1 to 3 [10, 11, 13–21, 35, 36]
2. The number of water layers present sometimes exceeds the value of W/S [14,15]
3. The reported dependence of W_{bound} on W/S is not uniform, being quadratic in one case [14] and complex (higher than a fifth-power dependence!) in other cases [18, 20]
4. Curve-fitting-based hydration numbers vary widely: 3.5 [14–16], 6.7 [19], and 12 [20].

We now address the results obtained. There are two alternative interpretations of the results shown in Fig. 2

1. The two peaks obtained by curve fitting at about 2550 cm^{-1} and at about 2405 cm^{-1} correspond to different types of water in the pool, namely to W_{bound} and $W_{bulklike}$, respectively.

2. There is one type of water present, which gives rise to the observed main peak. The small peak need not be associated with HOD molecules present in a layer of different structure, as implied by the multistate water-solubilization model.

If the former model were correct then one would expect a correlation – that agrees with chemistry – between areas of the two peaks and W/S. The combined hydration numbers of Ca^{2+} and HSO_3^- (a model for the surfactant anion) is 9 ± 1 [37]. Accordingly, the fraction of W_{bound} should level off at a W/S value of about 9; this is not observed in Fig. 3C. Indeed, the fact that the ratio between the areas of both peaks is independent of W/S, to within 1%, argues against any model based on discrete structures of the aggregate-solubilized water.

A corollary to the discussion in the preceding paragraph is that the assumption that each of the bands which are obtained by curve fitting of ν_{OH} (of solubilized pure H_2O) or ν_{OD} (of solubilized pure D_2O) may be attributed to a different type of water is an oversimplification because these bands may originate from coupled water molecule vibrations and from a bending overtone often reported in the spectra of bulk H_2O and D_2O [35, 36, 38]. On the other hand, deconvolution of ν_{OH} or ν_{OD} vibrations of HOD is straightforward because both frequencies are essentially decoupled, provided that the concentration of D_2O is less than 10% [24, 32]. This advantage has been recognized both for the bulk aqueous phase [24, 25, 32] and for reverse aggregates [10, 11, 16, 36]. We used a small Gaussian peak in order to get a better fit (Fig. 2A). This use need not be associated with a second type of water within the pool because the ν_{OD} peak is asymmetric, as given elsewhere [24, 25, 35, 36, 38]. That is, our IR data are best explained without resorting to the coexistence of structurally different water layers within the pool.

We now turn our attention to the ^{1}H NMR data. Both for solubilized water and the surfactant methine proton (H1), Fig. 4 shows no discontinuity at W/S = 9, the threshold of formation of a W/O μE. A similar result was obtained for the methylene protons (H2, results not shown). Such a break is expected due to the formation of a new type of water, $W_{bulklike}$.

We employed the dependence of δ_{obs} of solubilized H_2O–D_2O mixtures on their deuterium content to calculate the deuterium/protium fractionation factor, φ_M, for micelle-solubilized water. Calculation of this factor from NMR data has been discussed elsewhere [12, 22], so only essential details will be covered. The micellar water pool is surrounded by a monolayer of surfactant molecules, so it is akin to a concentrated electrolyte solution. In the case of a W/O μE, applying the two-state water-solubilization model, taking into account the fact that water in the second layer is described as bulklike water, φ_M is given by

$$\varphi_M = (D/H)_{\text{bound water}}/(D/H)_{\text{bulklike water}} \quad . \tag{2}$$

The equation that is used to calculate φ_M. from ^{1}H NMR data is given by

$$(\delta_{HD} - \delta_H)/(\delta_D - \delta_H) = \{\varphi_M/[(1 - \chi_D) + \varphi_M\chi_D]\}\chi_D \quad , \tag{3}$$

where δ_{HD}, δ_H, and δ_D refer to the observed chemical shifts for a μE-solubilized H_2O–D_2O mixture, pure H_2O, and pure D_2O, respectively, and χ_D is the atom fraction of deuterium in the aggregate-solubilized water. It is customary to obtain δ_D by regression from plots of δ_{obs} versus χ_D; this is a straight line in the present case. A plot of the left-hand term of Eq. (3) versus χ_D should be linear for $\varphi_M = 1$, curve down for $\varphi_M < 1$, or curve up for $\varphi_M > 1$; this has been verified experimentally [12, 22].

The next step is to show how the value of φ_M can be interpreted in terms of the structure of reverse-aggregate-solubilized water relative to bulk water, whose fractionation factor is unity by definition. In a system where D and H equilibrate among a number of different sites, corresponding to different structures (bound and bulklike water in the present case) deuterium accumulate, relative to protiums, at sites where they are most closely confined by potential barriers. Therefore, $\varphi_M < 1$ implies a greater preference for deuterium in micellar bulklike water than in surfactant-bound water. The converse of this argument shows that $\varphi_M > 1$ is associated with stronger binding potentials in surfactant-bound water than in micellar bulk-like water. Because the two-state water-solubilization model implies that water in the first layer is more structured that in the second layer, *the fractionation factor for the aggregate-solubilized water is expected to be greater than unity*.

The result of the application of Eq. (3) to our ^{1}H NMR data is shown in Fig. 5. The plot is perfectly linear, CC = 0.9997, ΣQ = 0.016, which does not agree with a multilayer water-solubilization model. In discussing the meaning of this result, the following points should be borne in mind.

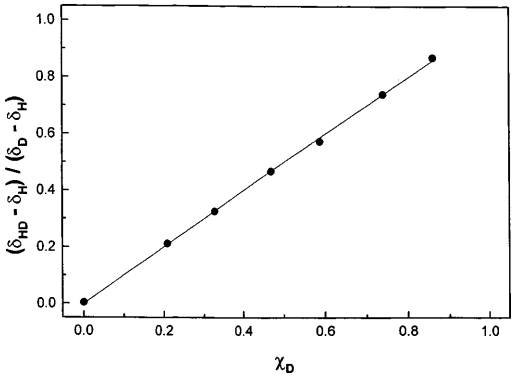

Fig. 5 Determination of the fractionation factor for $(EtHxSS)_2Ca$-solubilized water according to Eq. (3). Surfactant concentration = 0.2 M in C_6D_6; W/S = 18.09; T = 29.0 °C. The values of δ_H and δ_D are 2485.67 and 2478.49 Hz, respectively. For the plot shown CC = 0.9997 and ΣQ = 0.016

1. As shown by Eq. (2), the fractionation factor is an equilibrium constant, i.e., fast diffusion of water molecules between the different sites in the system (e.g., between bound and bulklike water, if present), and has no bearing on the calculation of φ_M.

2. Although fractionation factors, like other secondary isotope effects, are close to unity, they can be measured with high precision by NMR spectroscopy. For example, differences in φ as small as 1% have been reported [12, 22, 39]. Additionally, if we take W/S = 9 as the threshold of formation of a W/O μE (vide supra), then 50% of solubilized water should have been present as bound water, and D/H fractionation should have occurred, leading to $\varphi_M > 1$. Therefore, the unity fractionation factor obtained in the present work is neither due to a lack of sensitivity of the experimental technique nor, if one accepts the two-state solubilization model, to the presence of a negligible fraction of the more structured water.

3. The power of this technique is that calculation of φ_M and the consequent conclusion regarding the nature of aggregate-solubilized water do not require a preconceived model of water structure.

4. We emphasize that the unity fractionation factor which we obtained for $(EtHxSS)_2Ca$-solubilized water does not mean that it is similar to bulk water (for which $\varphi = 1$ by definition). It means, however, that we did not detect the coexistence of two, or more, water layers within the water pool which are structurally different (as implied by the two-state solubilization model) allowing D/H fractionation to occur, which should have resulted in $\varphi_M > 1$.

The results of both techniques indicate that treatment of experimental data in terms of the coexistence of

structurally different water "layers" within the pool is probably an oversimplification. Water seems to be present as one microphase whose properties change continuously as more water is solublized. At high W/S these properties are akin to, but not equal to, those of water in electrolyte solutions. This conclusion agrees with IR and NMR studies of water within reverse aggregates of ionic and nonionic surfactants [9–12, 35, 36], fluorescence measurements in RMs [40], NMR studies of concentrated salt solutions [41], IR results of HOD in bulk aqueous phases [27–29], theoretical calculations on the molecular dynamics of water [42], dielectric relaxation of water in hydrated phospholipid bilayers [43], and measurement of water chemical potentials in the presence of phospholipid bilayer membranes [44].

The following factors possibly contribute to an averaging of the water structure over the whole volume of the aqueous nanodroplet.

1. Water within the pool is confined to such a small volume that it is highly likely that each molecule is simultaneously affected by several neighboring headgroups, especially because the ionic interface fluctuates [45]. This may preclude the formation of water "layers" within the nanodroplet.

2. Surfactant monomers migrate from the W/O interface into the water pool [3]; this migration contributes to an averaging of the water structure because of hydrophobic hydration of the surfactant tail [46].

3. Water solubilization changes the relative stability, i.e., the population of different conformers of the sulfonate and the ester headgroups, these conformers bind water differently [20, 36].

Conclusions

We have used noninvasive techniques to investigate the state of solubilized HOD in RMs and W/O μEs of $(EtHxSS)_2Ca$. Although curve fitting of the ν_{OD} band required the use of two peaks, the relationship between individual peak areas and W/S does not support a multilayer structural model. The calculated fractionation factor also points in the same direction; therefore, IR and NMR results indicate that treatment of experimental data in terms of the coexistence of structurally different water layers within the pool is an oversimplification. The change in the slope of the graphs of certain physical properties as a function of increasing W/S, which is sometimes observed at the threshold of the formation of the W/O μE, may well reflect the expected decrease in water–surfactant interactions after completion of the hydration of the headgroup. Factors responsible for averaging of the water structure within the pool are discussed. The present results agree with those based on the use of other techniques, particularly NMR, in which information regarding the state of solubilized water (based on φ_M) *does not rely on a preconceived model of water structure*.

Acknowledgments L.P. Novaki thanks FAPESP for a postdoctoral fellowship, O.A. El Seoud thanks FAPESP for financial support and CNPq for a research productivity fellowship. We thank Paulo R. Olivato for making the FT-IR spectrophotometer (purchased with FAPESP funds) available to us.

References

1. Fendler, JH (1982) Membrane mimetic chemistry. Wiley, New York
2. Attwood D, Florence AT (1984) Surfactant systems: their chemistry, pharmacy, and biology. Chapman and Hall, London
3. Eicke H-F, Kvita P (1984) In: Luisi LP, Straub BE (eds) Reverse micelles: biological and technological relevance of amphiphilic structures in apolar media. Plenum, New York, p 21
4. Langevin D (1984) In: Luisi LP, Straub BE (eds) Reverse micelles: biological and technological relevance of amphiphilic structures in apolar media. Plenum, New York, p 287
5. (a) Candau F, Leong YS, Poyet G, Candau SJ (1984) J Colloid Interface Sci 101:167; (b) Candau F, Leong YS, Fitch RM (1985) J Polym Sci 23:195; (c) Candau F, Zekhini Z, Durand JP (1986) J Colloid Interface Sci 114:398
6. Kon-no K, Kitatahara A, El Seoud OA (1987) In: Schick M (ed) Nonionic surfactants: physical chemistry, Dekker, New York, p 185
7. (a) Goba RD, Kon-no K, Kandori K, Kitahara A (1983) J Colloid Interface Sci 93:293; (b) Lianos P, Thomas JK (1986) J Colloid Interface Sci 117:505
8. El Seoud OA (1994) In: Hinsze WL (ed) Organized assemblies in chemical analysis, vol. 1, JAI Press, Greenwich, p 7
9. (a) El Seoud OA, El Seoud MI, Mickiewicz JA (1994) J Colloid Interface Sci 163:87; (b) El Seoud OA, Okano LT, Novaki LP, Barlow GK (1996) Ber Bunsenges Phys Chem 100:1147
10. Novaki LP, El Seoud OA (1997) Ber Bunsenges Phys Chem 101:1928
11. Novaki LP, El Seoud OA (1998) J Colloid Interface Sci 202:391
12. (a) El Seoud OA (1997) J Mol Liq 72:85; (b) El Seoud OA, Novaki LP (1998) Prog Colloid Polym Sci 109:42
13. (a) Yoshioka H (1983) J Colloid Interface Sci 95:81; (b) Yoshioka H, Kazama S (1983) J Colloid Interface Sci 95:240; (c) Goto A, Yoshioka H, Kishimoto H, Fujita T (1992) Langmuir 8:441
14. Onori G, Santucci A (1993) J Phys Chem 97:5340
15. D'Angelo M, Onori G, Santucci A (1994) J Phys Chem 98:3189
16. Amico P, D'Angelo M, Onori G, Santucci A (1995) Nuovo Cimento D17:1053
17. (a) Boicelli CA, Giomini M, Giuliani, AM (1984) Appl Spectrosc 38:537; (b) MacDonald H, Bedwell B, Gulari E (1986) Langmuir 2:704; (c) Aliotta F, Migliardo P, Donato DI, Liveri VT, Bardez E, Larry B (1992) Prog Colloid Polym Sci 89:258

18. D'Aprano A, Lizzio A, Liveri VT, Aliotta F, Vasi C, Migliardo P (1988) J Phys Chem 92:4436
19. Giammona G, Goffredi F, Liveri VT, Vassallo G (1992) J Colloid Interface Sci 152:465
20. Jain TK, Varshney M, Maitra A (1989) J Phys Chem 93:7409
21. Maitra A, Jain TK, Shervani Z (1990) Colloids Surf 47:255
22. Schowen KB (1978) In: Gandour RD, Schowen RL (eds) Transition states for biochemical processes. Plenum, New York, p 225
23. Compton SV, Compton DAC (1993) In: Coleman PB (ed) Practical sampling techniques in infrared analysis, CRC Press, Boca Raton, p 217
24. Mundy WC, Gutierrez L, Spedding FH (1973) J Chem Phys 59:2173
25. (a) Wiafe-Akenten J, Bansil R (1983) J Chem Phys 78:7132; (b) Mikenda W (1986) Monatsh Chem 117:977; (c) Lindgren J, Hermansson K, Wójcik MJ (1993) J Phys Chem 97:5254
26. Derome A (1987) In: Baldwin JE (ed) Modern NMR techniques for chemistry research. Organic Chemistry Series. vol 6. Pergamon Press, Oxford, p 32
27. Waldron RD (1957) J Chem Phys 26:809
28. Wall TT, Hornig DF (1965) J Chem Phys 43:2079
29. Wall TT, Hornig DF (1967) J Chem Phys 47:784
30. (a) Walrafen GE (1968) J Chem Phys 48:244; (b) Schiffer J, Hornig DF (1968) J Chem Phys 49:4150; (c) Lucas M, De Trobriand A, Ceccaldi M (1975) J Phys Chem 79:913; (d) Kristiansson O, Eriksson A, Lindberg J (1984) Acta Chem Scand A 38:609
31. (a) Senior WA, Verrall RE (1969) J Phys Chem 73:4242; (b) Tiddy GJT (1979) Nucl Magn Reson 8:174; (c) Tiddy GJT (1980) Phys Rep 57:1
32. Wills HA, van der Maas JH, Miller RGJ (1987) Laboratory methods in vibrational spectroscopy, 3rd edn. Wiley, New York
33. (a) Maddams WF (1980) Appl Spectrosc 34:245; (b) Vandeginste BGM, De Galan L (1975) Anal Chem 47:2124
34. Gandour RD, Coyne M, Stella VJ, Schowen RL (1980) J Org Chem 45:1733
35. Pacynko WF, Yarwood J, Tiddy GJT (1987) Liq Cryst 2:201
36. Christopher DJ, Yarwood J, Belton PS, Hills B (1992) J Colloid Interface Sci 152:465
37. (a) Ohtaki H, Radani T (1993) Chem Rev 93:1157; (b) Marcus Y (1994) Biophys Chem 51:111; (c) Enderby JE, Neilson GW (1979) In: Franks F Water-a comprehensive treatise, vol 6 Plenum, New York, p 411
38. (a) Efimov YY, Naberukhin YI (1978) Mol Phy 36:973; (b) Scherer JR (1986) In: Clark RJ, Hester RE (eds) Advances in Infrared Raman spectroscopy, vol. 5, Wiley, New York, p 149; (c) Monosmith WB, Walrafen GE (1984) J Chem Phys 81:669; (d) Sokolowska A, Kecki Z (1986) J Raman Spectrosc 17:29; (e) Sokolowska A (1991) J Raman spectrosc 22:31; (f) Carey DM, Korenowski GM (1998) J Chem Phys 108:2669
39. (a) Jarret RM, Saunders M (1985) J Am Chem Soc 107:2648; (b) Jarret RM, Saunders M (1986) J Am Chem Soc 108:7549
40. (a) Belletête M, Droucher GJ (1989) J Colloid Interface Sci 134:289; (b) Belletête M, Lachapelle M, Droucher G (1990) J Phys Chem 94:5337
41. (a) Boden N, Mortimer M (1978) J Chem Soc Faraday Trans 2 74:353; (b) Baianu IC, Boden M, Lightowlers D, Mortimer M (1978) Chem Phys Letts 54:169
42. Teleman O, Joensson B, Engstroem S (1987) Mol Phys 60:193
43. Enders H, Nimtz G (1984) Ber Bunseges Phys Chem 88:512
44. Lis LJ, McAlister M, Fuller N, Rand RP, Parsegian VA (1982) Biophys J 37:657
45. Leonidis EB, Hatton TA (1989) Langmuir 5:741
46. Nakayama H, Yamanobe M, Baba K (1991) Bull Chem Soc Jpn 64:3023